Interface confinement and local structure in nc-Si/a-SiN_X multilayers (nc≡nanocrystalline, a≡amorphous)

2001 J. Phys.: Condens. Matter 13 9857

(http://iopscience.iop.org/0953-8984/13/44/303)

INSTITUTE OF PHYSICS PUBLISHING JOURNAL OF PHYSICS: CONDENSED MATTER

J. Phys.: Condens. Matter **13** (2001) 9857–9865 PII: S0953-8984(01)25088-7

Interface confinement and local structure in nc-Si/a-SiN$_x$ multilayers (nc $\equiv$ nanocrystalline, a $\equiv$ amorphous)

Li Wang[1,3], Xiaowei Wang[1], Xinfan Huang[1], Zhifeng Li[2], Zhongyuan Ma[1], Lin Zhang[1], Yun Bao[1], Jianjun Shi[1], Wei Li[1], Xiaohui Huang[1], Jun Xu[1] and Kunji Chen[1]

[1] National Laboratory of Solid State Microstructures and Department of Physics, Nanjing University, Nanjing 210093, People's Republic of China
[2] National Laboratory of Infrared Physics, Chinese Academy of Science, Shanghai 200083, People's Republic of China

Received 21 May 2001, in final form 19 July 2001
Published 19 October 2001
Online at stacks.iop.org/JPhysCM/13/9857

Abstract

The local structure of ultrathin a-Si:H sublayers embedded in a-Si:H/a-SiN$_x$:H multilayers before and after thermal annealing is investigated by Raman scattering spectroscopy. It is found that the confinement of the interfaces leads to a higher temperature being needed for crystallization of the multilayer with thinner a-Si sublayers. The local structure of a-Si becomes more disordered in the uncrystallized multilayer upon thermal annealing due to H-atom expulsion. The transverse optical mode of the residual a-Si shows a shift to high frequencies in peak position with a sharpening of the peak for the nc-Si/a-SiN$_x$ multilayers with increasing annealing temperature, which means that the network of a-Si tends to become more ordered. This tendency is not induced by the stress created during the thermal annealing but caused by the relaxation of the a-Si network.

1. Introduction

Observations of efficient photoluminescence (PL) from nanoporous Si and Si nanoparticles at room temperature have stimulated considerable research interest in the development of low-dimensional Si as a promising candidate for application in Si-based optoelectronics [1–3]. Among the many kinds of Si nanostructure, nanocrystalline silicon (nc-Si)/SiO$_2$ and nc-Si/hydrogenated amorphous silicon nitride (a-SiN$_x$:H) multilayers have attracted wide attention since the size of nc-Si produced can be precisely controlled. Moreover, blue-shifts of the photoluminescence and electroluminescence due to the quantum-size effect have been clearly observed for nc-Si/a-SiN$_x$:H superlattices [4, 5]. Recently, ordering and self-organization of

[3] Author to whom any correspondence should be addressed.

nc-Si has also been found in nc-Si/SiO_2 superlattices [6]. Many works have been done on electrical and optical properties of nc-Si/SiO_2 and nc-Si/a-SiN_x:H superlattices [7–9]. But the details of the structural change of ultrathin a-Si:H embedded in these multilayers that occurs upon annealing are not clearly understood.

The Raman scattering technique is widely employed to investigate local disorder and strain, and the resultant optical, electronic, and vibrational properties. It can provide information important for understanding the relation of lattice microstructure to other physical properties that depend on the local coordination. The optical phonon band of Si single crystal is narrow and is located at 520 cm^{-1}. When the size of Si crystallites is smaller than 10 nm, the Raman phonon band broadens and shifts down in energy with the decrease of the size of the Si crystallites due to the phonon confinement effect [10]. Also, the increased disorder in amorphous Si results in much stronger perturbation of the Raman phonon band, shifting it to 460–480 cm^{-1}. Raman experiments are conventionally performed with thick films. To our knowledge, although a few works on Raman scattering measurements of a-Si/SiO_2 and a-Si/a-SiN_x:H multilayers have been reported [11, 12], vibrational data on the local structure change of the ultrathin a-Si sublayers within these multilayers that occurs upon thermal treatment are less abundant.

In this work, we utilized Raman scattering spectroscopy to investigate the structural change of the a-Si:H/a-Si_x:H multilayers that occurs upon thermal treatment. It is found that in this system, the higher temperature needed for crystallization of the multilayers compared to thick a-Si:H is due to the confinement effect modulated by two a-Si/SiN_x:H interfaces. Moreover, upon thermal treatment, the local structure of the a-Si:H sublayer became more disordered when the annealing temperature was below the crystallization temperature; when the annealing temperature was higher than the crystallization temperature, the crystallization process occurred and nc-Si was formed, but a few areas of a-Si remained within which the local structure tended to be more ordered.

2. Experimental procedure

The nine-period a-Si:H/a-SiN_x:H multilayers were deposited on substrates of fused silica at 250 °C by a computer-controlled plasma-enhanced chemical vapour deposition (PECVD) system. The decomposition of silane and silane/ammonia was carried out at 200–300 mTorr with a rf power of 30 W. The Si sublayer thickness, D, varied from 2 to 4 nm. The a-SiN_x:H thickness was kept at 10 nm. Insulating a-SiN_x:H was fabricated with a gas mixture of $NH_3/SiH_4 = 5$ (volume ratio) and its band gap is about 3.0 eV. The recrystallization in samples was performed by rapid (30–90 s) thermal annealing (RTA) at 700–900 °C or furnace annealing at 1000 °C for 30 min in a N_2 environment.

The Raman measurements were done on a Jobin-Yvon LabRam INFINITY micro-Raman system with excitation by the 514.5 nm line of an Ar^+ laser in back-scattering geometry with a liquid-nitrogen-cooled CCD detector. The transmission electron microscopy (TEM) measurements were performed with JEM200CX microscope working at 200 kV. A Fourier transform infrared (FTIR) spectroscope (Nicolet 170SX) was employed to record the bonding configurations of the sample before and after thermal annealing.

3. Results and discussion

Figure 1 shows the Raman spectra of the as-deposited sample and the samples annealed at different temperatures for the same time, 70 s. The as-deposited Si layers are amorphous

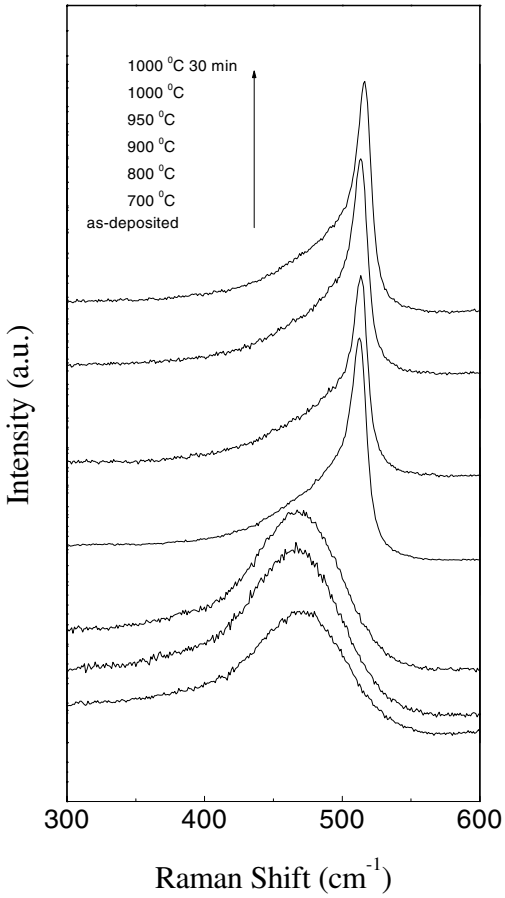

Figure 1. Raman spectra of the samples with $D = 4$ nm annealed at various temperatures for 70 s.

as confirmed by the broad Raman scattering band at 473 cm^{-1}. The broad a-Si-like band is still present in the Raman spectra of the samples annealed at 700 °C and 800 °C, but the peak position has shifted slightly to lower frequency. This means that the structures of the a-Si sublayers in the multilayers annealed at 700 and 800 °C are different to that for the as-deposited sample, although the Si sublayers in the annealed samples remain amorphous. However, upon thermal annealing at 900 °C, a sharp peak at 514 cm^{-1} ascribed to the TO mode of nc-Si, with a weak shoulder corresponding to a-Si, emerges in the spectrum, which demonstrates that nc-Si has formed in the sample. The features of the spectra of the samples annealed at 950 °C and 1000 °C are quite similar to those of the spectrum of the sample annealed at 900 °C. In addition to the c-Si-like band, the a-Si-like band is still present in the spectra, even for the sample that has undergone furnace annealing at 1000 °C for 30 min. This means that after thermal annealing treatment, a few areas of a-Si:H remain in the samples, although a great quantity of nc-Si is formed. Above all, it is found that the crystallization temperature in this work approaches the value 1273 K reported in reference [13] but is higher than that for thick a-Si films, about 650 °C. As we will reveal later, the reason that a higher temperature is needed for crystallization of our samples compared with that for the thick a-Si films is the confinement of the Si/SiN$_x$ interfaces.

Figure 2 is a cross-sectional TEM micrograph of the sample which was prepared with a 4 nm thick a-Si sublayer, after it had been annealed at 900 °C for 50 s using RTA. One can see that nc-Si is formed within initially a-Si sublayers, which is consistent with the Raman observation. The flat and abrupt interfaces between a-Si and a-SiN_x remain after thermal annealing, and, in addition, the a-SiN_x sublayers show no obvious changes. As was mentioned in the experimental section, the optical band gap of the a-SiN_x sublayers is about 3.0 eV. The N content x is estimated to be 1.3, indicating that the a-SiN_x that we fabricated approaches stoichiometry [14]. Thus, no Si or N atoms can aggregate due to the stability of the SiN sublayers during the thermal annealing processes. Moreover, the thicknesses of the Si and SiN_x sublayers in the annealed samples show no changes and are still consistent with the original values. TEM observations reveal that the nc-Si/a-SiN_x multilayers can be obtained by thermally annealing a-Si:H /a-SiN_x:H and the amount of nc-Si produced can be controlled by changing the sizes of the initial a-Si:H sublayers.

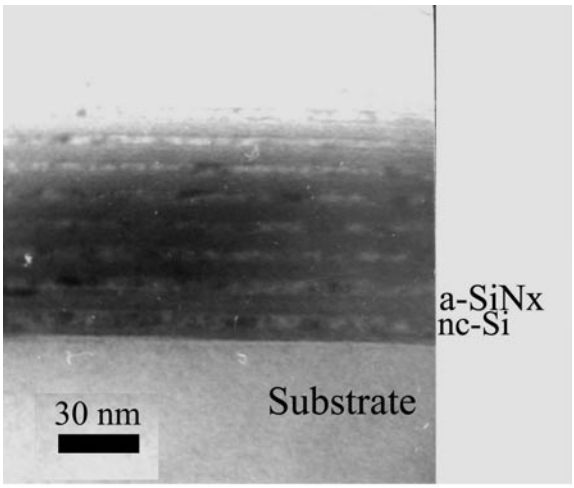

Figure 2. The cross-sectional TEM micrograph of the sample with $D = 4$ annealed at 900 °C for 50 s.

For the samples with the thinner Si layers ($D = 2$ or 3 nm), no signal of nc-Si can be detected from the samples after annealing at $\leqslant$1000 °C. After RTA at 1000 °C, all samples exhibit partial crystallization and the proportion of a-Si phase is greater for the thinner Si sublayers, as shown in figure 3. The diffusion of N atoms during thermal annealing will inhibit the crystallization of a-Si. To clarify the influence of N diffusion, we analysed the microstructure of the annealed samples by TEM. The cross-sectional TEM micrograph of the annealed samples shows that a-SiN_x sublayers exhibit no obvious change and the interfaces are kept flat and abrupt, indicating that few N atoms can move during the thermal annealing. Wang *et al* reported that atoms bonded at or near the interface have distorted bonding arrangements in a-Si/SiO_2 multilayers due to the presence of the interfaces [11]. The crystallization mainly occurs and progresses in the 'bulk' region of a-Si far away from the interfaces. In our multilayer case, except for the areas near the interfaces, the narrow space with the thin a-Si sublayer far from the interfaces impedes the occurrence of crystallization. Therefore, in the multilayers with the thinner sublayers, the confinement modulated by the interfaces becomes more pronounced, so the progression of the crystallization becomes more difficult. Thus it is reasonable that a higher temperature is needed to realize the crystallization for the thinner a-Si sublayers.

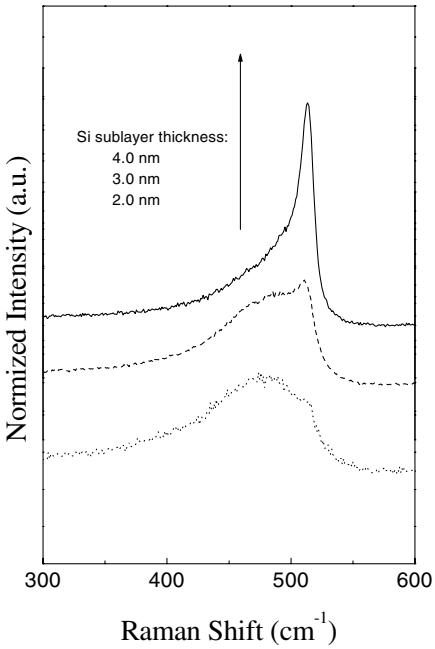

Figure 3. Raman spectra of the samples annealed at 1000 °C for 70 s; $D = 4$ nm: solid line; $D = 3$ nm: dashed line; $D = 2$ nm: dotted line.

To understand the local structure change of the a-Si:H sublayer during the thermal annealing, we will focus on the change of the transverse optical (TO) mode in a-Si:H. Its band peak position P_{TO} can be treated as a measure of the average strain or pressure resulting from disorder; in this paper, its bandwidth—using the full width at half-maximum (FWHM)—is found to be sensitive to local disorder and correlates with rms deviations in the bond angle, $\delta\theta$, from the ideal tetrahedral bond angle of 109.4° in a-Si. Beeman *et al* pointed out that the rms bond-angle deviation $\delta\theta$ is the appropriate parameter for characterizing the structural changes [15]. Also, they calculated the dependence of $\delta\theta$ on the linewidth of the TO mode on the basis of various model structures. It can be described as $\Delta_{TO} = 15 + 6\,\delta\theta$. To minimize the influence of the weak vibrational modes, we performed a best fit on each spectrum from 300 to 600 cm^{-1}, to (i) three a-Si-like bands and a straight line for the uncrystallized samples and (ii) three a-Si-like bands, one c-Si-like band, one microcrystalline state and a straight line for the crystallized samples. Without the microcrystalline state band, the fitted curve does not show good agreement with the experimental curves.

The fitted parameters for the TO vibrational mode of a-Si in the annealed samples are given in figure 4. The peak position and FWHM of the TO mode for the as-deposited sample are obtained as 474.1 cm^{-1} and 56.0 cm^{-1}, respectively. From figure 4, one can see that a slight red-shift of the peak position and a slight broadening of the bandwidth of the TO mode for the uncrystallized samples compared with those for as-deposited films, such as the samples annealed at 700 or 800 °C, are observed. This means that the a-Si:H sublayers in these samples become more disordered.

Ishidate *et al* reported that the FWHM of the TO band in a-Si:H films decreases monotonically with the increasing H concentration [16]. Hence, we utilized Fourier transform infrared spectroscopy (FTIR) to investigate the bonding configurations of the samples with 4 nm

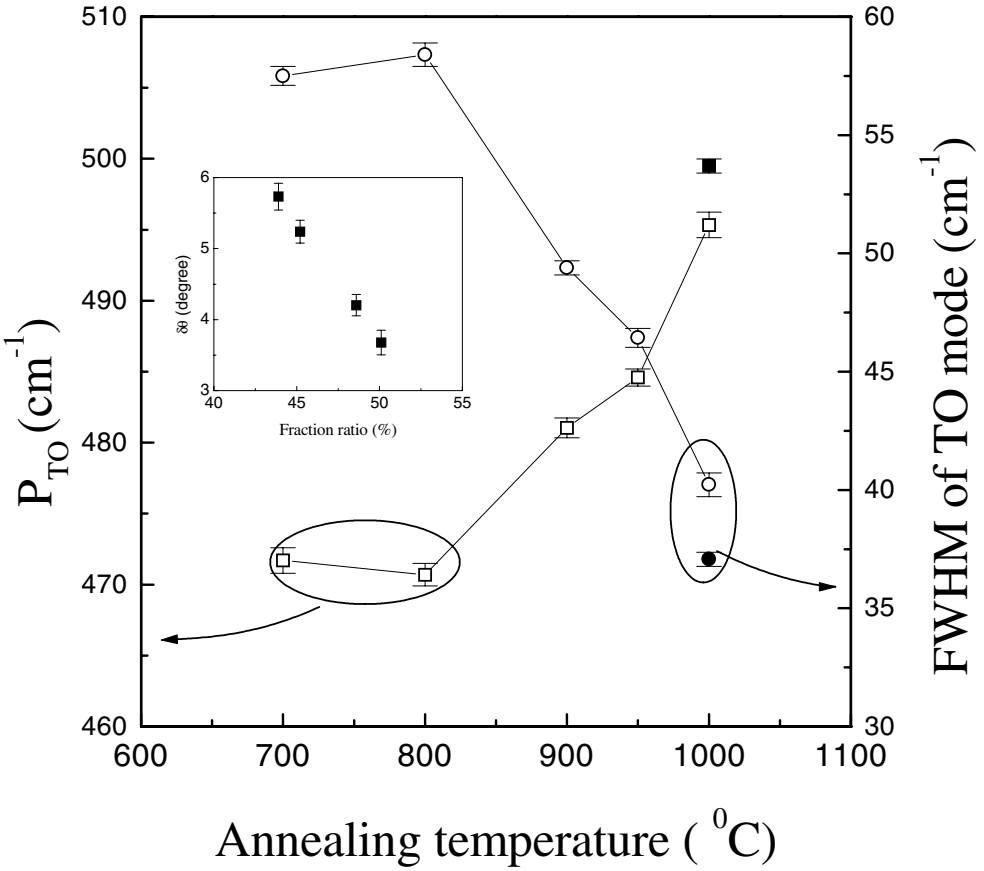

Figure 4. P_{TO} and FWHM versus annealing temperature for the sample with $D = 4$ nm. Squares are for P_{TO}; circles are for the FWHM. Open symbols are for the samples annealed by rapid thermal processes; solid symbols are for the sample annealed at 1000 °C for 30 min. The lines are drawn through the data points to guide the eye. The inset shows the rms bond-angle deviation ($\delta\theta$) versus crystallinity fraction curve.

thick a-Si sublayers before and after thermal annealing, as shown in figure 5. In figure 5(a), the spectrum of the as-deposited sample, three major bands are observed; the 800–900, 2000–2240 and 2800–3000 cm^{-1} bands can be attributed to the Si–N, Si–H and N–H stretching modes [17]. The Si–H and N–H bands weaken upon annealing at 450 °C for 70 s. In the sample annealed at 1000 °C for 70 s, we found that H-related bonds disappeared from the annealed samples. Thus, we consider that the broadening of the FWHM of the TO mode for the annealed samples is due to the H expulsion during the thermal annealing processes.

Let us discuss the local structure of the residual a-Si in the sample after the crystallization process has occurred. First, the peak positions of the a-Si TO mode for the crystallized samples shift to higher frequencies and the FWHM of the a-Si TO mode in the crystallized samples becomes narrower compared with those for the as-deposited samples. Second, from figure 4, it is clear that the peak positions of the a-Si TO mode shift to higher frequencies with increasing annealing temperature and approach the maximum value 495.3 cm^{-1} for the sample that has undergone furnace annealing at 1000 °C for 30 min. At the same time, the FWHM of the TO mode varies from 49.4 cm^{-1} at 900 °C to 40.2 cm^{-1} at 1000 °C. The estimated

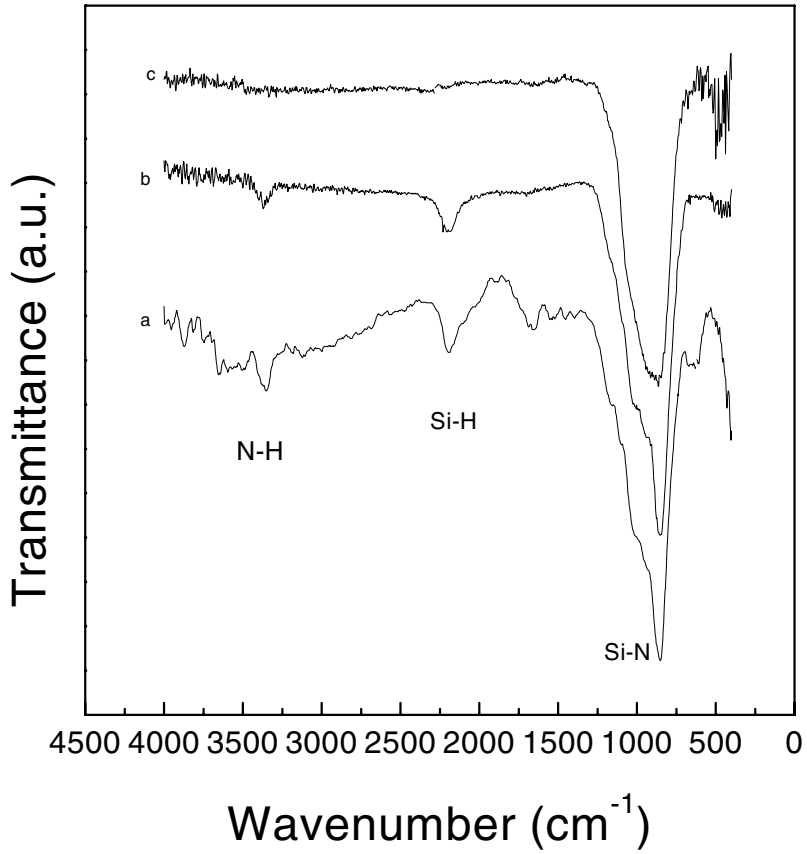

Figure 5. FTIR spectra of the samples with a 4 nm thick a-Si sublayers before and after thermal annealing: (a) the as-deposited sample; (b) the sample annealed at 450 °C for 70 s; (c) the sample annealed at 1000 °C for 70 s.

rms bond-angle derivation $\delta\theta$ decreases from 5.7° to 3.7° with increase of the annealing temperature. Meanwhile, we calculated the fractions of nc-Si in the different samples, defining the crystallinity fraction ratio $[I_c]/([I_c] + [I_a])$ where I_c and I_a are the integrated areas of the TO bands of nc-Si and a-Si, respectively. The fraction increases monotonically from 43.9% in the sample annealed at 900 °C for 70 s to 50.3% in the sample annealed at 1000 °C for 30 min. It is found that there is a linear correlation between the fraction and $\delta\theta$, as shown in the inset of figure 4. This means that the network of a-Si becomes more ordered with the presence of more nc-Si.

P_{TO} and the FWHM for the samples annealed at 900 °C for different times are given in figure 6. The TO band shows a shift in peak position to higher frequencies with a sharpening of the peak (reduction of the width) when the annealing time increases. Also, the fraction in the samples varies from 39.7% at 30 s to 43.9% at 70 s. $\delta\theta$ also decreases monotonically with the increase of the fraction.

This shifting to higher frequencies of P_{TO} and reduction of the FWHM with the increase of the fraction is similar to the pressure dependence of the TO band in plasma-deposited a-Si:H films. The TO band of a-Si:H shows a shift of the peak to higher frequencies with a reduction of the width when higher pressure is applied [16]. However, in our case, when a-Si

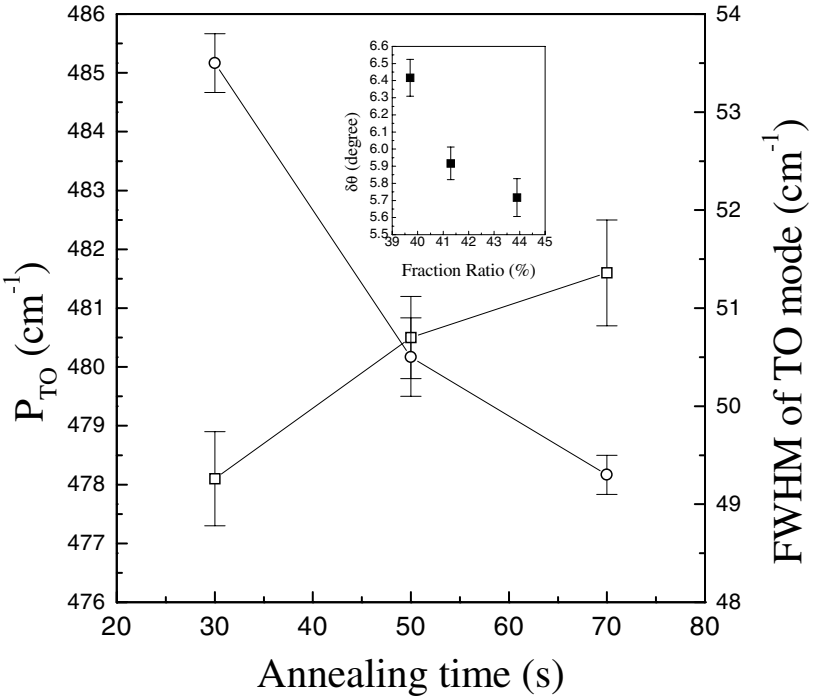

Figure 6. P_{TO} and FWHM versus the annealing time for the samples with $D = 4$ nm annealed at 900 °C. Squares are for P_{TO}; circles are for the FWHM. The lines are drawn through the data points to guide the eye. The inset shows the rms bond-angle deviation ($\delta\theta$) versus crystallinity fraction curve.

is transformed to c-Si, the volume becomes smaller; consequently, the network of the residual a-Si:H must be tensile but not compressed. Thus, the narrowing and upshift of the TO mode are not due to the presence of stress induced by the crystallization. So we tentatively suggest that they originate from the relaxation of the network of a-Si, as described in references [15] and [18]. The relaxed network is more ordered than the unrelaxed one and is advantageous to the crystallization processes, which is consistent with our observations, the coexistence of the more ordered network of a-Si and the formation of more nc-Si.

4. Conclusions

In conclusion, we utilized Raman scattering spectroscopy to investigate the structural change of the a-Si:H/a-Si_x:H multilayers that occurs upon rapid thermal treatment. It is found that in this system, the higher crystallization temperature needed for the multilayers compared to thick a-Si:H is due to the confinement effect modulated by two a-Si/SiN_x:H interfaces. Upon thermal treatment, the local structure of the a-Si:H sublayer became more disordered due to the H-atom expulsion during the thermal process when the annealing temperature was below the crystallization temperature; when the annealing temperature was higher than the crystallization temperature, the crystallization process occurred and nc-Si was formed, but a few areas of a-Si remained and its local structure tended to be more ordered. The tendency of a-Si to have a more ordered network is not induced by the stress created during the crystallization but originates from the relaxation of the a-Si network.

Acknowledgments

This work was supported by the National Natural Science Foundation of China (Grants No 69876019, No 69890225 and No 60071019) and partly supported by the NPTND of Korea MOST. One of the authors (L Wang) is grateful for the financial support of a Motorola fellowship.

References

[1] Canham L T 1990 *Appl. Phys. Lett.* **57** 1046
[2] Holmes J D, Johnston K P, Doty R C and Korgel B A 2000 *Science* **287** 1471
[3] Linros J, Lalic N, Galeckas A and Grivickas V 1999 *J. Appl. Phys.* **86** 6128
[4] Chen K, Huang X, Xu J and Feng D 1992 *Appl. Phys. Lett.* **61** 2069
[5] Wang M, Huang X, Xu J, Li W, Liu Z and Chen K 1998 *Appl. Phys. Lett.* **72** 722
[6] Grem G F, Lockwood D J, McCaffrey J P, Labbe H J, Fauchet P M, White B Jr, Diener J, Kovalev D, Koch F and Tsybeskov L 2000 *Nature* **407** 358
[7] Ma Z, Liao X, Kong G and Chu J 1999 *Appl. Phys. Lett.* **75** 1857
[8] Tsybeskov L, Hirschman K, Duttagupta S, Zacharias M, Fauchet P, McCaffrey J P and Lockwood D 1998 *Appl. Phys. Lett.* **72** 43
[9] Khriachtchev L, Kilpela O, Karirinne S, Keranen J and Lepisto T 2001 *Appl. Phys. Lett.* **78** 323
[10] Ritcher H, Wang Z and Ley L 1981 *Solid State Commun.* **58** 739
[11] Wang Y, Matsuda O, Serikawa T and Murase K 2000 *J. Physique* IV **10** 259
[12] Khriachtchev L, Novikov S and Kilpela O 2000 *J. Appl. Phys.* **87** 7805
[13] Zacharias M, Blasing J, Veit P, Tsybeskov L, Hirschman K and Fauchet P M 1999 *Appl. Phys. Lett.* **74** 2614
[14] Volodin V, Efremov M, Gritsenko V and Kochubei S 1998 *Appl. Phys. Lett.* **74** 1212
[15] Beeman D, Tsu R and Thorpe M F 1985 *Phys. Rev.* B **32** 32 874
[16] Ishidate T, Inoue K, Tsuji K and Minomura S 1982 *Solid State Commun.* **42** 197
[17] Seol K, Futami T, Watanabe T, Ohki Y and Takiyama M 1999 *J. Appl. Phys.* **85** 6746
[18] Spinella C, Lombardo S and Priolo F 1998 *J. Appl. Phys.* **84** 5383